the cost of reduced energy production. So, it appears that, ICL is essential for *M. tuberculosis* under normal conditions of growth, the importance of which may be increased in conditions of stress related to dormancy, such as nutrient depletion and anerobic metabolism.

As mentioned earlier, ICL from various bacteria and other organisms has been isolated and biochemically characterized. From these observations, the molecular weight of ICL ranges from a very high value of 123 kDa in *Turbatrix aceti*, a free-living nematode[16], to a low value of 44.7 kDa in *E. coli*[17]. Our observation is that *M. tuberculosis* ICL has a molecular weight in the range of 90 kDa.

The *aceA* gene encoding ICL, is part of the *aceBAK* operon in *E. coli*. *aceB* encodes malate synthase and *aceK* encodes isocitrate dehydrogenase kinase/phosphatase. In *E. coli* it has been observed that the operon employs a single promoter upstream of *aceB*. It is interesting to note that the expression of *aceK* is downstream of *aceA* gene. It is possible that the competitor enzyme isocitrate dehydrogenase could be regulated by ICL. But in the case of *M. tuberculosis* H37Rv, the organization of this operon seems to be different. From a careful analysis of the genome sequence, it is apparent that *aceB* is situated very far from *aceA*.

Recently Kerstin *et al.*[18], have characterized the activity and expression of ICL in *M. avium* and *M. tuberculosis* by using two-dimensional gel electrophoresis, of the several proteins expressed by *M. avium* in the intracellular environment. They have reported that only *M. tuberculosis* strain CSU93 expressed detectable levels of *aceA* and not H37Rv. But we have cloned and expressed *aceA* gene of *M. tuberculosis* H37Rv.

Several proteins like crystalline homologue[19], 27 kDa protein[20] and enzymes like alanine dehydrogenase[21] have been implicated in dormancy.

We therefore concur with the earlier workers that dormancy in *M. tuberculosis* may be controlled by more than one mechanism and further research in this field is necessary to draw a clear-cut conclusion as to how and what exactly triggers dormancy and to see whether ICL has a role to play in dormancy.

1. Report on the tuberculosis epidemic 1997, World Health Organization, WHO, Geneva, 1997.
2. Kochi, A., *Immunobiology*, 1994, **191**, 235–236.
3. Gupta, U. D. and Katoch, V. M., *Indian J. Lepr.*, 1997, **69**, 385–393.
4. Kannan, K. B., Katoch, V. M., Bharadwaj, V. P., Sharma, V. D., Datta, A. K. and Shivannavar, C. T., *Indian J. Lepr.*, 1985, **572**, 542–548.
5. Bharadwaj, V. P., Katoch, V. M., Sharma, V. D., Kannann, K. B., Datta, A. K. and Shivannavar, C. T., *Indian J. Lepr.*, 1987, **59**, 158–162.
6. Wheeler, P. R. and Ratledge, C., *Br. Med. Bull.*, 1988, **44**, 547–561.
7. Murthy, P. S., Sirsi, M. and Ramakrishnan, R., *Am. Rev. Respir. Dis.*, 1973, **108**, 689–690.
8. Seshadri, R., Murthy, P. S. and Venketasubramanian, T. A., *Indian J. Biochem. Biophys.*, 1976, **13**, 95–96.
9. Wayne, L. G. and Lin, K. Y., *Infect. Immunol.*, 1982, **37**, 1042–1049.
10. Birnboim, H. C. and Dolly, J., *Nucleic Acids Res.*, 1979, **7**, 1513–1523.
11. McFadden, B. A., *Methods Enzymol.*, 1969, **13**, 163.
12. Narayanan, S., Sahadevan, R., Ramanujam, S. and Narayanan, P. R., *Indian J. Tuberc.*, 1992, **40**, 99–105.
13. Cole, S. T. *et al.*, *Nature*, 1998, **393**, 537–544.
14. Andrejew, A., *Ann. Inst. Pasteur*, 1948, **74**, 464–466.
15. Nyka, W., *Infect. Immunol.*, 1974, **9**, 843–850.
16. Reiss, U. and Rothstein, M., *Biochemistry*, 1974, **13**, 1796–1800.
17. Mackintosh, C. and Nimmo, H. G., *Biochem. J.*, 1988, **250**, 25–31.
18. Kerstin Honer Zu Bentrup, Andras Miczak, Dana K. Swenson and David G. Russell, *J. Bacteriol.*, 1999, **181**, 7161–7167.
19. Cunningham, A. F. and Spreadbury, C. L., *J. Bacteriol.*, 1998, **180**, 801–808.
20. Lee, B. H., Murugasu-Oei, B. and Dick, T., *Mol. Gen. Genet.*, 1998, **260**, 475–479.
21. Hutter, B. and Dick, T., *FEMS Microbiol. Lett.*, 1998, **167**, 7–11.

ACKNOWLEDGEMENT. Financial assistance in the form of a Senior Research Fellowship to the first author from Council of Scientific and Industrial Research, New Delhi, is acknowledged.

Received 15 July 2000; revised accepted 6 October 2000

Digital analysis of induced erythrocyte shape changes in hypercholesterolemia under *in vitro* conditions

M. Manjunatha and Megha Singh*

Biomedical Engineering Division, Indian Institute of Technology, Chennai 600 036, India

Under *in vitro* conditions, the incubation of normal erythrocytes in cholesterol-enriched plasma (CEP) for half, one, and two hours leads to increase in the membrane cholesterol level, whereas there is no change in phospholipids composition. This excessive accumulation of cholesterol leads to shape alteration in erythrocytes as observed by phase-contrast microscope. For quantification, these images after digitization are processed to obtain perimeter, area and form factor. These parameters are used to quantify the changes in the shape of erythrocytes induced by hypercholesterolemic process.

THERE are several *in vivo* mechanisms, which induce changes in erythrocyte membrane lipids and proteins and their interior, leading to alteration in erythrocyte shape, which in turn affects the deformability[1–5]. Such changes under *in vitro* conditions are also observed in erythrocytes

*For correspondence.

the cost of reduced energy production. So, it appears that, ICL is essential for *M. tuberculosis* under normal conditions of growth, the importance of which may be increased in conditions of stress related to dormancy, such as nutrient depletion and anerobic metabolism.

As mentioned earlier, ICL from various bacteria and other organisms has been isolated and biochemically characterized. From these observations, the molecular weight of ICL ranges from a very high value of 123 kDa in *Turbatrix aceti*, a free-living nematode[16], to a low value of 44.7 kDa in *E. coli*[17]. Our observation is that *M. tuberculosis* ICL has a molecular weight in the range of 90 kDa.

The *aceA* gene encoding ICL, is part of the *aceBAK* operon in *E. coli*. *aceB* encodes malate synthase and *aceK* encodes isocitrate dehydrogenase kinase/phosphatase. In *E. coli* it has been observed that the operon employs a single promoter upstream of *aceB*. It is interesting to note that the expression of *aceK* is downstream of *aceA* gene. It is possible that the competitor enzyme isocitrate dehydrogenase could be regulated by ICL. But in the case of *M. tuberculosis* H37Rv, the organization of this operon seems to be different. From a careful analysis of the genome sequence, it is apparent that *aceB* is situated very far from *aceA*.

Recently Kerstin *et al.*[18], have characterized the activity and expression of ICL in *M. avium* and *M. tuberculosis* by using two-dimensional gel electrophoresis, of the several proteins expressed by *M. avium* in the intracellular environment. They have reported that only *M. tuberculosis* strain CSU93 expressed detectable levels of *aceA* and not H37Rv. But we have cloned and expressed *aceA* gene of *M. tuberculosis* H37Rv.

Several proteins like crystalline homologue[19], 27 kDa protein[20] and enzymes like alanine dehydrogenase[21] have been implicated in dormancy.

We therefore concur with the earlier workers that dormancy in *M. tuberculosis* may be controlled by more than one mechanism and further research in this field is necessary to draw a clear-cut conclusion as to how and what exactly triggers dormancy and to see whether ICL has a role to play in dormancy.

1. Report on the tuberculosis epidemic 1997, World Health Organization, WHO, Geneva, 1997.
2. Kochi, A., *Immunobiology*, 1994, **191**, 235–236.
3. Gupta, U. D. and Katoch, V. M., *Indian J. Lepr.*, 1997, **69**, 385–393.
4. Kannan, K. B., Katoch, V. M., Bharadwaj, V. P., Sharma, V. D., Datta, A. K. and Shivannavar, C. T., *Indian J. Lepr.*, 1985, **572**, 542–548.
5. Bharadwaj, V. P., Katoch, V. M., Sharma, V. D., Kannann, K. B., Datta, A. K. and Shivannavar, C. T., *Indian J. Lepr.*, 1987, **59**, 158–162.
6. Wheeler, P. R. and Ratledge, C., *Br. Med. Bull.*, 1988, **44**, 547–561.
7. Murthy, P. S., Sirsi, M. and Ramakrishnan, R., *Am. Rev. Respir. Dis.*, 1973, **108**, 689–690.
8. Seshadri, R., Murthy, P. S. and Venketasubramanian, T. A., *Indian J. Biochem. Biophys.*, 1976, **13**, 95–96.
9. Wayne, L. G. and Lin, K. Y., *Infect. Immunol.*, 1982, **37**, 1042–1049.
10. Birnboim, H. C. and Dolly, J., *Nucleic Acids Res.*, 1979, **7**, 1513–1523.
11. McFadden, B. A., *Methods Enzymol.*, 1969, **13**, 163.
12. Narayanan, S., Sahadevan, R., Ramanujam, S. and Narayanan, P. R., *Indian J. Tuberc.*, 1992, **40**, 99–105.
13. Cole, S. T. *et al.*, *Nature*, 1998, **393**, 537–544.
14. Andrejew, A., *Ann. Inst. Pasteur*, 1948, **74**, 464–466.
15. Nyka, W., *Infect. Immunol.*, 1974, **9**, 843–850.
16. Reiss, U. and Rothstein, M., *Biochemistry*, 1974, **13**, 1796–1800.
17. Mackintosh, C. and Nimmo, H. G., *Biochem. J.*, 1988, **250**, 25–31.
18. Kerstin Honer Zu Bentrup, Andras Miczak, Dana K. Swenson and David G. Russell, *J. Bacteriol.*, 1999, **181**, 7161–7167.
19. Cunningham, A. F. and Spreadbury, C. L., *J. Bacteriol.*, 1998, **180**, 801–808.
20. Lee, B. H., Murugasu-Oei, B. and Dick, T., *Mol. Gen. Genet.*, 1998, **260**, 475–479.
21. Hutter, B. and Dick, T., *FEMS Microbiol. Lett.*, 1998, **167**, 7–11.

ACKNOWLEDGEMENT. Financial assistance in the form of a Senior Research Fellowship to the first author from Council of Scientific and Industrial Research, New Delhi, is acknowledged.

Received 15 July 2000; revised accepted 6 October 2000

Digital analysis of induced erythrocyte shape changes in hypercholesterolemia under *in vitro* conditions

M. Manjunatha and Megha Singh*

Biomedical Engineering Division, Indian Institute of Technology, Chennai 600 036, India

Under *in vitro* conditions, the incubation of normal erythrocytes in cholesterol-enriched plasma (CEP) for half, one, and two hours leads to increase in the membrane cholesterol level, whereas there is no change in phospholipids composition. This excessive accumulation of cholesterol leads to shape alteration in erythrocytes as observed by phase-contrast microscope. For quantification, these images after digitization are processed to obtain perimeter, area and form factor. These parameters are used to quantify the changes in the shape of erythrocytes induced by hypercholesterolemic process.

THERE are several *in vivo* mechanisms, which induce changes in erythrocyte membrane lipids and proteins and their interior, leading to alteration in erythrocyte shape, which in turn affects the deformability[1–5]. Such changes under *in vitro* conditions are also observed in erythrocytes

*For correspondence.

due to pH variation[6], incubation at high temperature[7], treatment with triton X100 and sodium salicylate[8] and during blood storage[9].

Hypercholesterolemic process induces changes in the erythrocyte membrane. This is primarily attributed to accumulation of cholesterol in the membrane[10]. This has been observed under *in vivo*[11–14] as well as *in vitro*[15,16] conditions. Gradual increase in plasma cholesterol in experimental rabbits, maintained on atherogenic diet, also led to its accumulation in arterial vessels[17,18]. These observations show that the gradual change in erythrocyte shape, as observed microscopically, may reflect the effect of cholesterol in the arterial vessels. For better identification of the induced changes, the erythrocyte images should be obtained and processed under standardized conditions.

Erythrocyte deformability is an inherent property attributed to the size and shape of these cells. Basically, the erythrocytes contain excess surface area than that required to hold their volume and thus allowing these cells to undergo various shape transformations while flowing through the cardiovascular system. Any deviation from the discoidal shape alters the deformability of these cells[10]. Hence variation in morphometric parameters such as surface area and perimeter may show the extent of changes in the flow properties of these cells.

Recent studies on the digital analysis of morphometric characteristics of erythrocytes show that such an analysis could be valuable in diagnosing coronary artery disease[19], to determine the effect of cholesterol in capillary flow[20], to monitor erythrocyte aggregation[21] and to detect changes in erythrocytes due to blood storage[9]. Thus the data on morphometric changes may prove to be of diagnostic value. To our knowledge such an analysis in induced hypercholesterolemia has not been reported todate. Hence, the objective of the present work is to determine the changes in surface area, perimeter and form factor of erythrocytes and to relate these with cholesterol to phospholipid (C/P) ratios of erythrocytes as obtained by incubating these cells in cholesterol-enriched plasma (CEP).

Fresh human blood was drawn by venepunture, in a test tube containing acid citrate dextrose (ACD) (10 : 1.3). By centrifuging the blood at 3000 rpm, the plasma was separated and buffy coat on the top of cells was removed and discarded. The cells were gently washed by mixing with buffered saline. After centrifugation, the supernatant layer was removed and discarded and cells separated. To increase the C/P ratio in cells, the washed erythrocytes were suspended in CEP[16] and incubated for 2 h at 37°C. During incubation, after 1/2 h and 1 h, the blood samples were removed. From these, the smears were prepared and dried in air. The same was repeated for erythrocyte suspension incubated for two hours and cells separated from the CEP were photographed by transmission-type phase contrast microscope at 1000X (Hertel and Reuss, Germany).

The C/P ratios in control plasma and erythrocytes were 0.79 and 0.81, respectively. In CEP this was increased to 1.39, whereas the increased values of this parameter in erythrocyte membranes incubated for half, one and two hours were 0.96, 1.02 and 1.08, respectively. Cholesterol and phospholipids of plasma, CEP and erythrocyte membrane were measured by the methods of Baginski and Zak[21] and Naito[22], respectively.

The images of the normal and cholesterol-enriched erythrocytes obtained by the above procedures were scanned using the ScanJet grey image scanner (software-dependent), with charge-coupled device image sensor, 16 level (4 bit) per picture element, with output resolution 38–600 dpi, selectable in one dpi increments digitized using the image processing system (Hewlett Packard, USA). From these, the images of ten cells of each category were grabbed and processed by using the MATLAB by median filtering[24], Sobel operator for edge enhancement, thresholding to obtain a binary image[25], median filtering and finally contour extraction[26]. The sequence of operations for the shape analysis of erythrocyte images obtained under *in vitro* conditions is given in Figure 1.

For calculation of area, the contour of the cell was filled up with pixels. By counting the number of these and

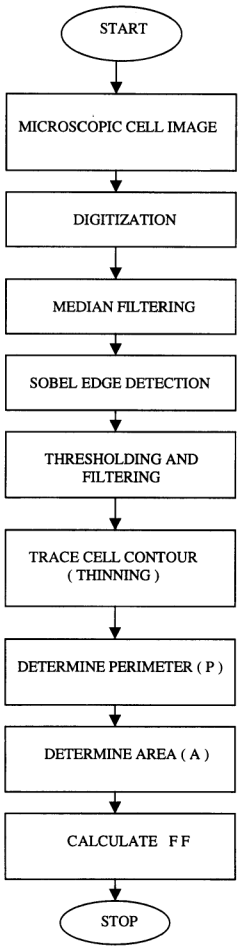

Figure 1. Sequence of operations applied to process the erythrocyte images.

multiplying with pixel area, the area (A) of the cell was determined. Similarly, by counting the number of pixels along the perimeter and then multiplying with pixel length, the perimeter (P) of the same cell was determined.

Based on these, the form factor (FF) = $P^2/4\pi A$ was calculated. This parameter is the measure of compactness or roundness of the cell and its variation indicates the deviation of the shape in the image from that of a disc (FF for disc = 1). The calibration of the above measurement procedure was carried out by determining area and perimeter of a circle of known diameter. This procedure was further verified with similar measurement of circles of known diameters. A good agreement between the measured and calculated values was obtained. Statistical analysis of the data was carried out by Student's t-test.

Figure 2 shows the images of the erythrocytes, normal and after incubation for half, one and two hours, as obtained by phase contrast microscope. The gradual changes in normal erythrocytes during cholesterol-enrichment up to two hours are clearly observed. Figure 3 shows the contour of the erythrocytes as obtained from the sequence of images by image processing procedures. A transition from discocytes to crenated erythrocytes as obtained by this process is attributed to cholesterol accumulation in the middle layer of the membrane[9]. Deviation from the discoid shape after half an hour shows the accumulation of cholesterol in the membrane. Further accumulation leads to distortion of the shape and finally crenation of the erythrocytes[10]. This alteration also results in change in the brightness of the central pallor, indicating that there is gradual transition from discocytes to acanthocytes/echinocytes[26].

The shape parameters (Table 1) show the respective variations. The area shows highly significant decrease with the increase of C/P of the erythrocyte membrane. In contrast to this, the perimeter shows a highly significant increase with the change in shape in erythrocytes. The crenated cells, after incubation for 2 h show minimum area and maximum perimeter compared to normal cells.

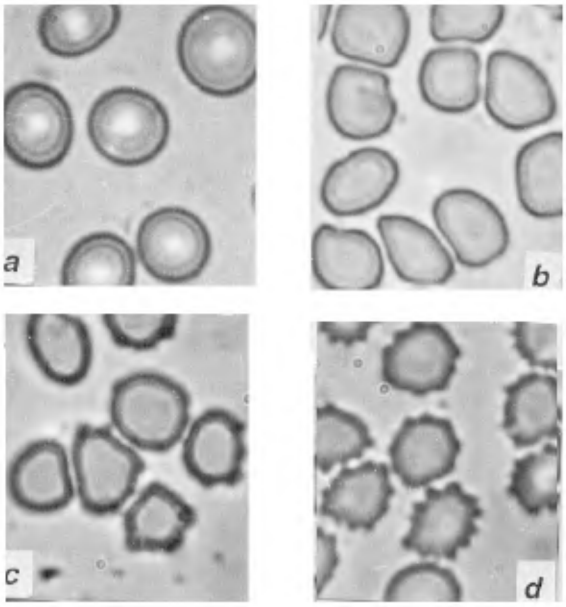

Figure 2. Images of erythrocytes as obtained by phase contrast microscope. ***a***, normal; and after incubation in cholesterol-enriched plasma for ***b***, $\frac{1}{2}$ h; ***c***, 1 h; and ***d***, 2 h.

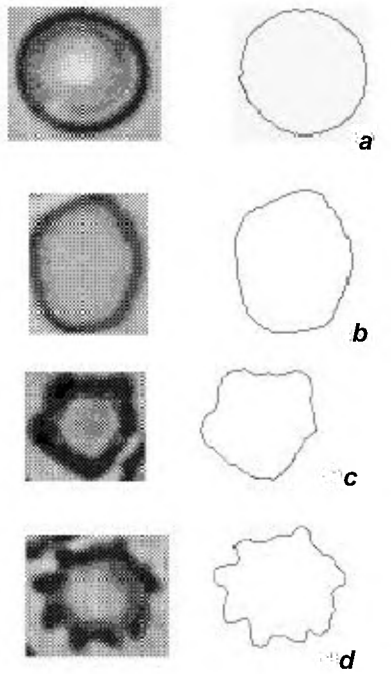

Figure 3. Shape and contours of erythrocytes. ***a***, normal; and after incubation for ***b***, $\frac{1}{2}$ h; ***c***, 1 h; and ***d***, 2 h.

Table 1. Shape parameters of normal and cholesterol-enriched erythrocytes after incubation in cholesterol-enriched plasma for $\frac{1}{2}$, 1 and 2 hours

	Erythrocytes			
		After incubation for		
Shape parameter	Normal	$\frac{1}{2}$ hour	1 hour	2 hour
Area, μm^2	$51.17 \pm 0.35^+$	49.92 ± 0.7*	47.85 ± 0.41*	46.85 ± 0.7*
Perimeter, μm	$25.5 \pm 0.35^+$	28.75 ± 0.47*	29.93 ± 0.69*	32 ± 1.44*
Form factor	$1.011 \pm 0.02^+$	1.31 ± 0.02*	1.48 ± 0.09*	1.738 ± 0.23*

+, Mean ± SD, *, $P < 0.0005$.